

Estimating Sediment Discharge Hydrographs in Downstream Rivers with a Large Amount of Sediment Yielded by a Heavy Rainfall

Shoji Fukuoka^{1*}, Takahisa Gotoh¹, Kotaro Okayasu²

1 Research and Development Initiative, Chuo University, Japan

2 Tosa Road Office, Shikoku Regional Development Bureau, MLIT, Japan

*Corresponding author, e-mail: sfuku@tamacc.chuo-u.ac.jp

Abstract

It is important to estimate the sediment discharge hydrograph during a flood with large amounts of sediment transports because the sediment discharge hydrograph gives an upstream boundary condition for the flood flow and bed variation analysis. In 1995, the record breaking largest flood of the Hime River occurred and brought a large-scale sediment depositions and channel migrations due to the flood. Those large-scale bed variations caused a levee breach and damages of river structures.

The study presented the concept of the bed variation analysis in rivers where main channel migrations and large-scale sediment depositions occurred due to a large amount of inflow sediment discharge from mountainous areas. The inflow sediment discharge hydrograph was estimated by the introduction of the new concept for the flood flow and bed variation analysis. The presented method was applied to 1995 flood of the Hime River and could reproduce the large-scale sediment depositions and the channel migrations due to the flood.

Keywords: Upstream sediment boundary condition, Sediment discharge hydrograph, Bed aggradation, Channel migration, Sediment yield

1 Introduction

The record breaking heavy rainfalls have caused large amounts of sediment yields in the upstream devastated mountainous basins and have brought sediments-related disasters in the lower reach of rivers. It is important to establish the estimation method for the sediment discharge hydrograph in rivers with a large amount of sediment yield during floods.

The Hime River basin contains the Itoigawa-Shizuoka Tectonic Line, in which has brought a large amount of sediment yields due to heavy rainfalls. The record breaking largest flood of the Hime River occurred in 1995. The flood caused large-scale sediment depositions and channel migrations in

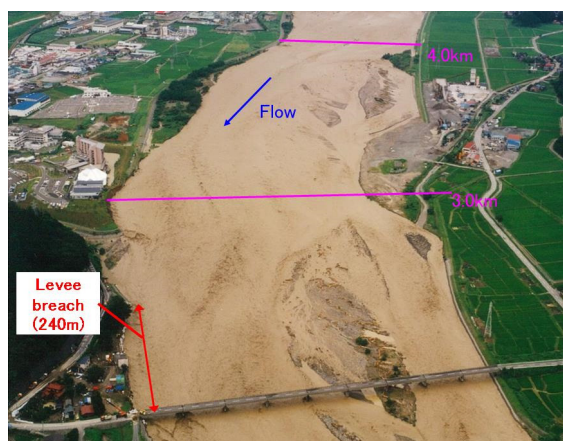


Figure.1 Aerial photo during 1995 flood in the Hime River

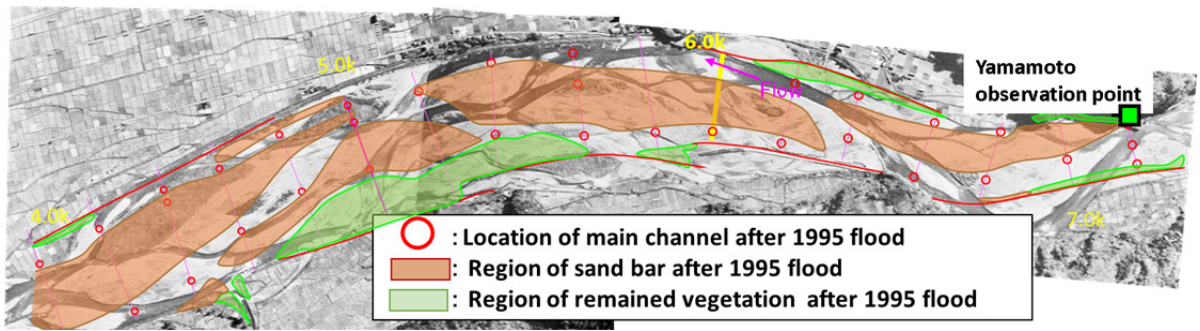


(a) Right after the 1995 flood around 4.0km

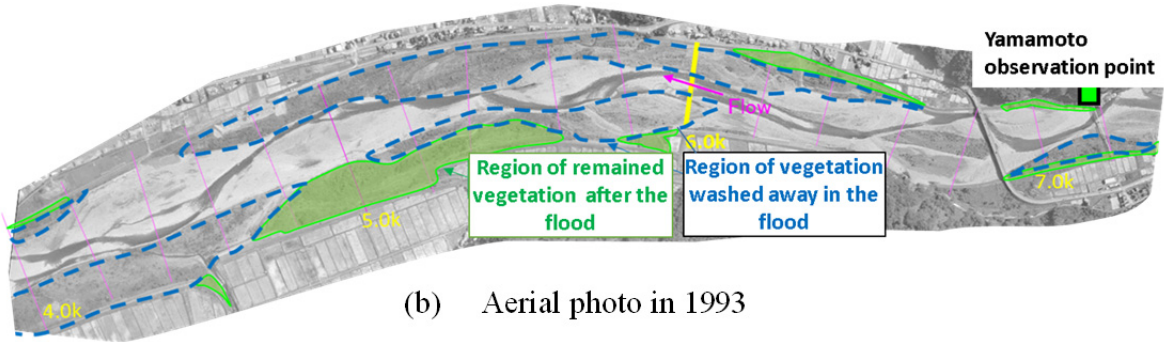


(b) In 2015 around 4.0km

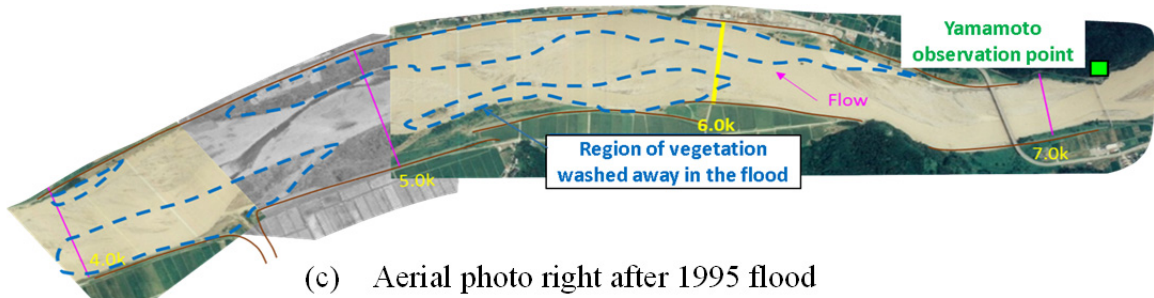
Figure.2 The situations that the bed materials became finer due to the large flood



(a) Aerial photo in 1947



(b) Aerial photo in 1993



(c) Aerial photo right after 1995 flood

Figure.3 Plan views of the river channels in 1947, 1993 and right after 1995 flood

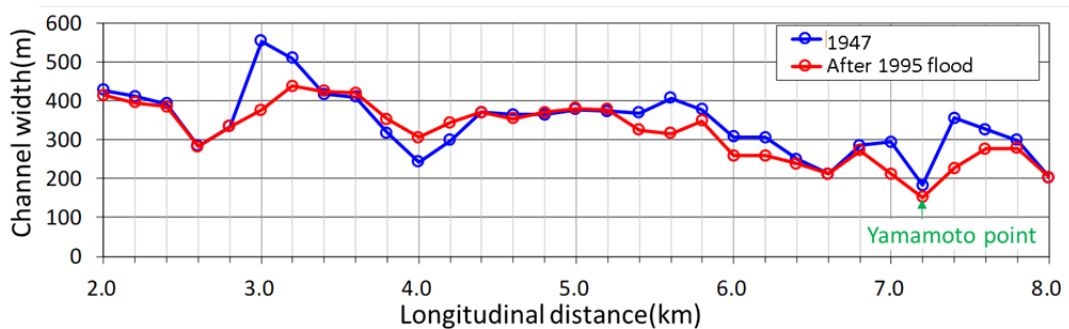


Figure.4 Longitudinal distribution of channel width in 1947 and after 1995 flood

the lower reach of the Hime River. And, the flood brought a levee breach and damages of river structures. Fig.1 shows the aerial photo during the 1995 flood. And Fig.2 shows river beds right after the 1995 flood in comparison with 2015 river beds. The bed materials right after the flood became finer due to the large amounts of fine sediments yielded from devastated mountainous areas. Fig.3(a) indicates regions of sandbar formations, remained vegetations and location of lowest bed elevation after the 1995 flood superposed on aerial photographs of 1947. And Fig.3(b) and Fig.3(c) indicate plan views of the river channel before and right after the flood. The straight main channel was formed in the middle of the river in 1993. However, the main channel after the 1995 flood meandered due to sandbar formations by the large-scale sediment depositions. Thus, a large amount of sediment deposition increases the risk of levee breaches. Fig.4 shows longitudinal distribution of channel width in 1947 and after the flood of 1995. The channel width and the meandering pattern of the main channel after the 1995 flood almost agree with those of the river channel in 1947. These

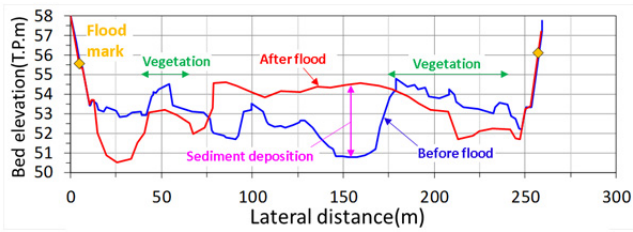


Figure.5 Change in the measured cross sectional shapes before and after the flood (6.0km)

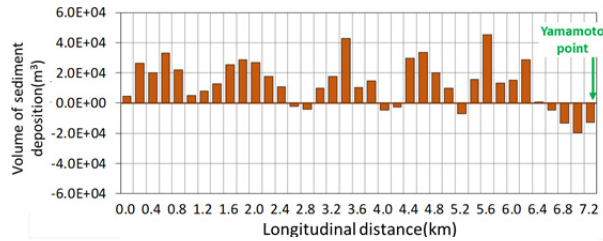


Figure.6 Longitudinal volume of the measured sediment deposition

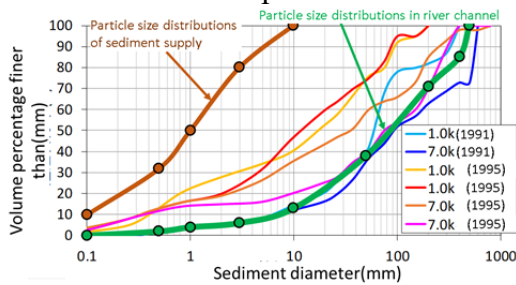


Figure.7 Change in the measured particle size distribution of sediment material before and after the flood

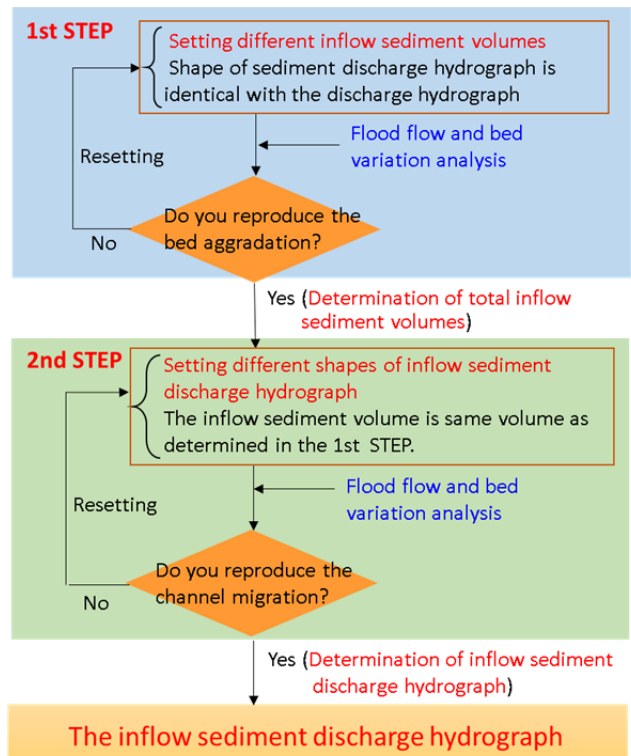


Figure.8 Estimation procedure for the inflow sediment discharge hydrograph

results demonstrate that when a flood accompanied by a large amount of sediments occurs, the channel width and the meandering patterns of the Hime River return to the state of the channel as shown in 1947.

In order to clarify the mechanism of flow and bed variation under such an extremely large flood, it is necessary to estimate the sediment discharge hydrographs which give the upstream boundary conditions of the flood flow and bed variation analysis. In general, the equilibrium sediment discharge or sediment concentrations by the empirical formulas have been given to the upstream boundary conditions for the flood flow and bed variation analysis. However, this method is not suitable for rivers with large amounts of sediment transports.

In this study, we presented the concept of bed variation analysis in rivers where channel migrations and large-scale sediment depositions occurred due to a large amount of inflow sediment discharge. And the sediment discharge hydrographs at an upstream boundary condition of the bed variation analysis was estimated based on the presented concept of the analysis. The presented method was applied to reproduce the large-scale bed aggradations and channel migrations of the 1995 flood in the Hime River with.

2 River bed aggradation and channel migration by July 1995 flood in the Hime River

Fig.5 shows the cross sectional shape of the river bed at 6.0km before and after 1995 flood. The main channel before the flood was located in the center of the channel. The main channel at the flood was shifted to the bank side. The river bed along the levee was scoured and the vegetation on the sandbars was washed away.

Fig.6 indicates a longitudinal volume of the sediment deposition measured after the flood. About 0.5 million m³ of sediments were deposited in the river reach from 0.0km to 7.2km by the flood. Fig.7 shows the particle size distributions before and after the flood. At 7.0km, sediment diameter of D60 was about 200 mm before the flood and varied to about 100mm after the flood. The large

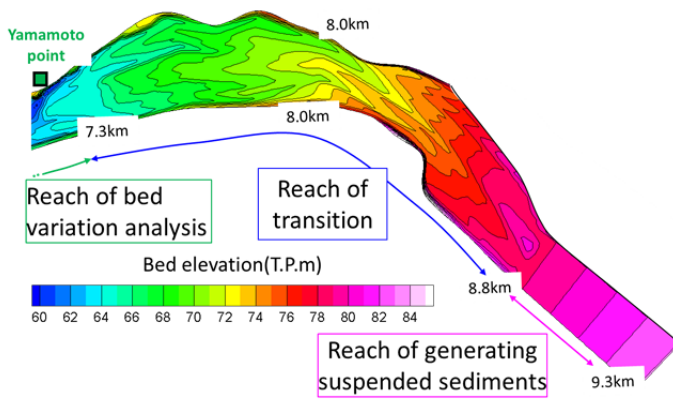


Figure.9 Calculation method of upstream boundary condition for the suspended sediment

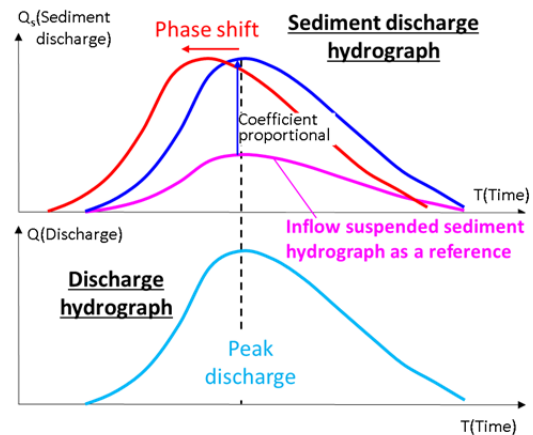


Figure.10 Concept of setting inflow suspended sediment discharge hydrograph

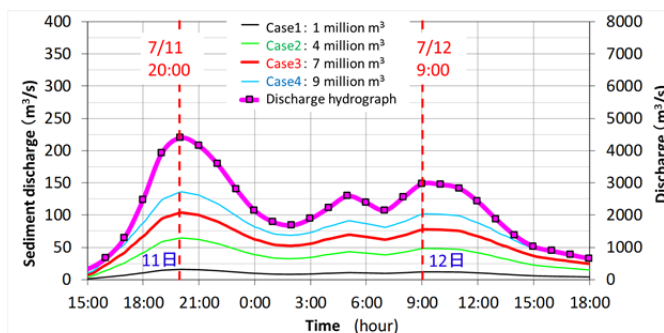


Figure.11 Discharge hydrograph and inflow sediment discharge hydrograph (the same shape as discharge hydrograph)

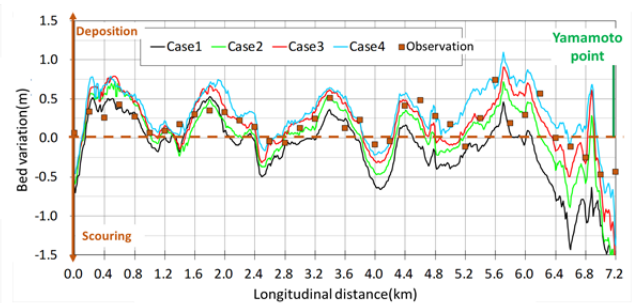


Figure.12 Longitudinal distributions of change in the measured and calculated mean bed elevation after the flood (Case1 to Case4)

amounts of fine sediments were deposited longitudinally in the main channel and shifted the thalweg from the middle of the channel to the levee side.

3 Concept of flood flow and bed variation analysis in rivers with a large amount of sediment transport

From Chapter 2, it was assumed that most of inflow sediments were fine and transported in suspension during the flood. The estimation of the suspended sediment discharge hydrograph at the upstream boundary is important to calculate the channel migrations and sediment depositions. It could be possible to estimate the inflow sediment discharge hydrograph by conducting flood flow and bed variation analysis in stages so as to agree with the observed and the calculated sediment deposition and channel migration after the flood. Fig.8 shows the estimation procedure of the inflow sediment discharge hydrograph. It is necessary to determine both the total inflow sediment volume and the shape of the hydrograph in order to estimate the inflow sediment discharge hydrograph. Thus, the estimation of inflow sediment hydrograph was conducted in two steps.

The first step was determination of the total inflow sediment discharge volume. The flood flow and bed variation analysis was conducted by setting different inflow sediment discharge volumes. And the inflow sediment volume was determined by reproducing the bed aggradation shown in Fig.6. The shape of the inflow sediment discharge hydrograph was the same as the shape of the discharge hydrograph.

The second step was determination of the shape of inflow sediment discharge hydrograph. The total inflow sediment volume was the value estimated in the first step, and the calculation was performed by setting different shapes of inflow sediment discharge hydrographs. The shape of the

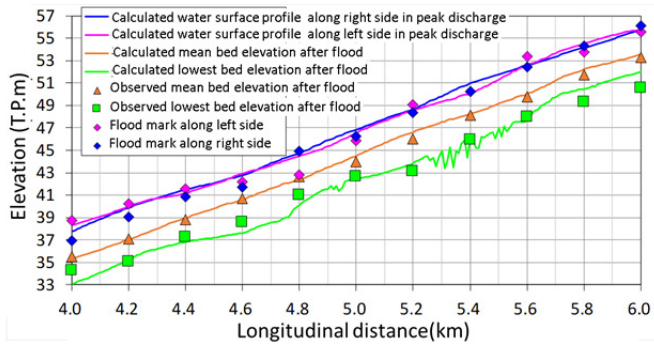


Figure.13 Observed and calculated water surface profiles and river bed profiles of Case3

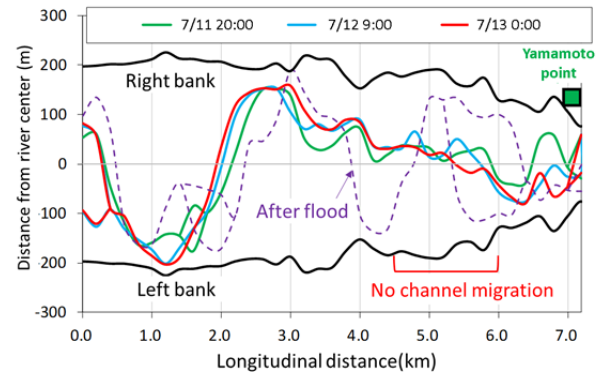


Figure.14 Observed loci of the main channel and calculated ones of Case3

inflow sediment discharge hydrograph was estimated by reproducing the observed bed aggradation and channel migrations after the flood.

4 Analysis of flood flow and bed variation considering a large amount of inflow sediment discharge

4.1 Calculation method and condition

The computation was performed in the reach from -0.6km to 7.3km. Fig.9 explains the calculation method of upstream boundary condition for suspended sediment transport analysis. At the upstream end, the reach for generating a large amount of suspended sediment transported from the upstream basin was set from 8.8km to 9.3km. The width and slope of this reach were given by the average river width and bed slope of the study area of the Hime River. The transition reach (7.3km to 8.8km) was installed between the suspended sediment generation reach and the bed variation calculation reach. The bed topography of the transition reach was given by the topography of the actual measured river channel. The suspended sediment discharge hydrograph was formed in the transition reach and supplied to the upstream boundary condition for the bed variation calculation in the downstream. Such a suspended sediment discharge hydrograph was assumed to be a unit suspended sediment discharge hydrograph. The inflow suspended sediment discharge hydrograph was determined by multiplying the proportional coefficient to the unit suspended sediment discharge hydrograph so as to agree with the measured downstream sediment deposition and channel migration after the flood. Fig.10 shows a schematic diagram of the inflow suspended sediment discharge hydrograph given at the upstream boundary.

The BVC method (Uchida and Fukuoka, 2014) was applied to calculate the three dimensional flows under complicated river conditions. The discharge hydrograph in Fig.11 obtained from the runoff analysis was given to the upstream boundary condition of the flood flow analysis. And the observed tidal levels at Toyama Bay was given to the downstream boundary condition. The two dimensional bed variation analysis was conducted and suspended sediment transports were calculated by the depth integrated two-dimensional advection diffusion equation of suspended sediment concentrations.

4.2 Estimation of inflow sediment discharge hydrograph

The first step shown in Fig.8 was performed for determination of the total inflow sediment discharge volume. Here, Hashinoki et al. (2007) reported that the sediment yielding volume in the upper mountainous basin in July 1995 flood was about 8.6 million m³. In our study, this value was referred to the inflow sediment volumes of Case1 to Case4. The shape of inflow sediment discharge hydrograph was the same as that of the discharge hydrograph. Four different inflow sediment volumes were given in Fig.11.

Fig.12 shows the measured and calculated results of changes in the mean bed elevations by the floods in Case1 to Case4. The calculation results of Case1 and Case2 were not able to reproduce the measured bed aggradation because of small inflow sediment volume. The results of Case4 showed

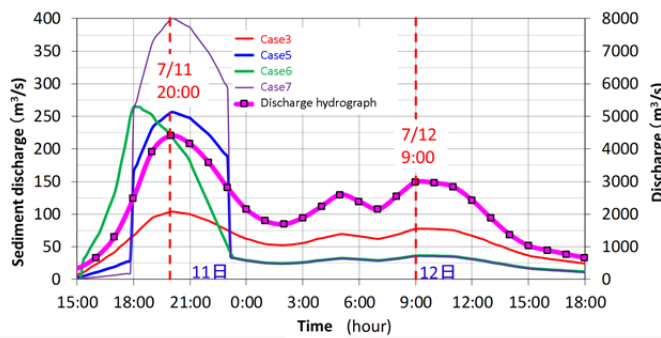


Figure.15 Inflow sediment discharge hydrographs

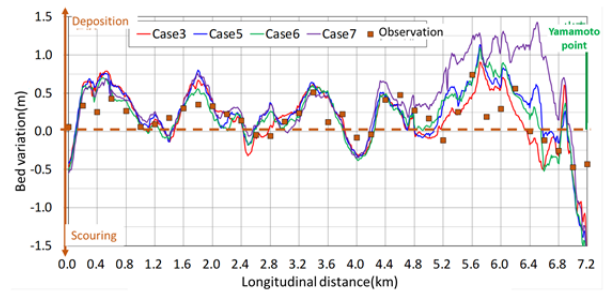


Figure.16 Longitudinal distributions of change in the measured and calculated mean bed elevation after the flood (Case3, Case5, Case6 and Case7)

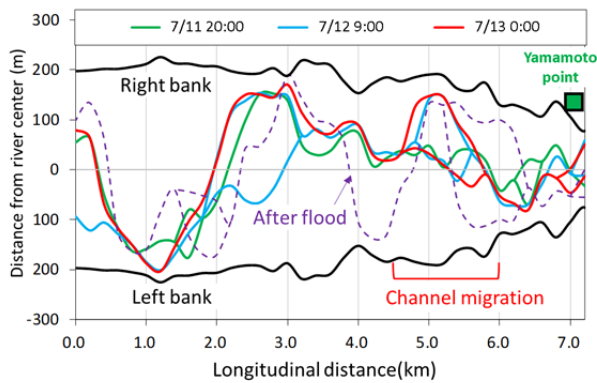


Figure.17 Observed loci of the main channel and calculated ones Case5

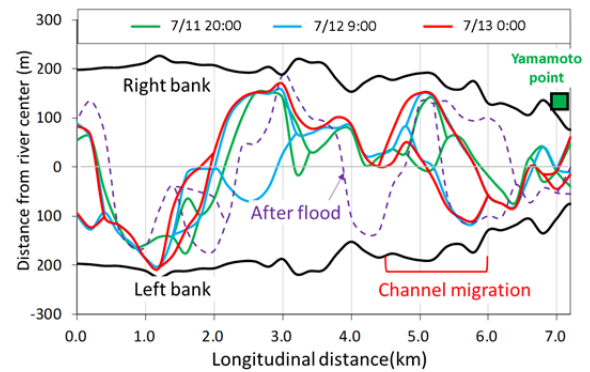


Figure.18 Observed loci of the main channel and calculated ones of Case6

that the calculated sediment depositions were larger than the measured one because the inflow sediment volume was too large. On the other hand, the results of Case3 in which the inflow sediment volume was about 7 million m^3 reproduced relatively the measured longitudinal sediment deposition. Fig.13 shows the comparison of the longitudinal observed flood marks and the calculated water surface profiles at the peak discharge in Case3. And the comparison between the observed and calculated longitudinal distributions of the bed elevation is also shown in Fig.13. The calculated water surface profiles and bed profiles almost explained the longitudinal distribution of the observed ones. From the above, it was demonstrated that the total inflow sediment volume that could reproduce longitudinal sediment deposition was about 7 million m^3 . Fig.14 shows the observed thalweg in the main channel after the flood and the temporal changes in the calculated thalweg of Case3. The main channel calculated in the Case3 still remained at the middle of the channel and the main channel did not shift to the levee as shown in the observed one.

The second step was performed for determination of the inflow sediment discharge hydrograph. Since landslides in the upper river basin occurred intensively at the time around the peak discharge (Hashinoki et.al., 2007), the inflow sediment discharge hydrograph of Case5 was assumed as shown in Fig.15. Furthermore, since the peak of suspended sediment discharge hydrograph generally occurs earlier than the flood peak discharge (Kinoshita, 1984), the peak of the inflow sediment discharge hydrograph which was two hours earlier than Case5 was assumed (Case6 in Fig.15). The total inflow sediment volume of Case5 and Case6 were about 7 million m^3 determined in the first step. And the total inflow sediment volume of Case7 was about 9 million m^3 with the same shape of hydrograph as Case6. Case7 was set to verify the total inflow sediment discharge volume obtained in the first step. Fig.16 shows the longitudinal distribution of the measured and calculated changes in mean bed elevations in Case5 to Case7 due to the flood. As in Case3, the results of Case5 and Case6 which the inflow sediment volume was about 7 million m^3 reproduced approximately the measured bed aggradation. However, in Case7 with an inflow sediment volume of about 9 million m^3 , the calculated longitudinal sediment depositions were larger than the measured one from 5.0km to 7.0km where the river width was wide. Therefore, it is found that the inflow sediment volume of

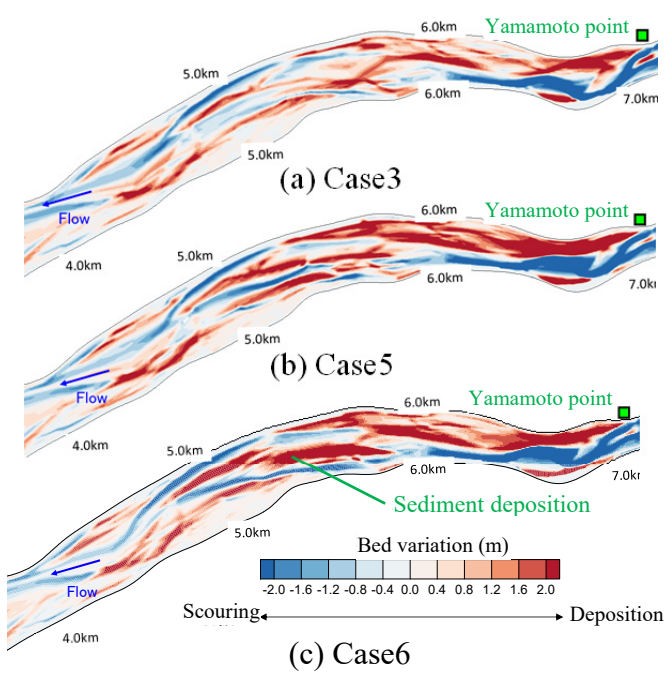


Figure.19 Calculated bed variations of Case3, Case5 and Case6

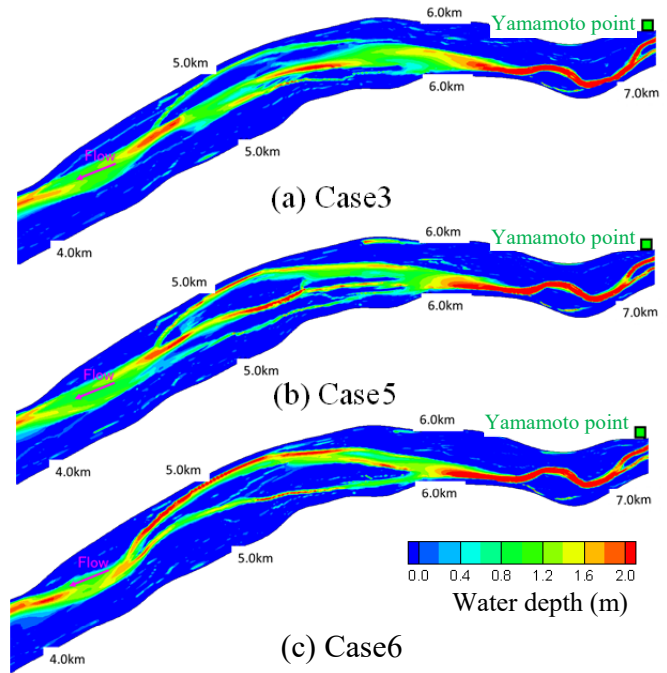


Figure.20 Calculated loci of the main channel of Case3, Case5 and Case6

approximately 7 million m^3 could reproduce the longitudinal distribution of the observed bed variations.

Fig.17 shows the observed thalweg in the main channel after the flood and the temporal changes in the calculated thalweg of Case5. In Case5, the migration of the main channel did not occur at the time of peak discharge (7/11 20:00), but at the time of second peak (7/12 9:00), the main channel shifted from the middle of the channel toward the left and right banks. And the main channel meandered as shown in Fig.17.

Fig.18 shows the observed thalweg in the main channel and the calculated thalweg of Case6. In Case6 where the peak of inflow sediment discharge hydrograph was 2 hours before the peak discharge, the main channel shifted from the middle of the river toward the left and right bank at the peak discharge (7/11 20:00). The results of Case 6 could reproduce that the main channel shifted toward the left and right banks in comparison with the results of Case 5. Fig.19 shows the contour of the calculated bed variations of Case3, Case5 and Case6, respectively. And Fig.20 shows the calculated main channel loci of Case3, Case5 and Case6. The main channel loci in Fig.20 were revealed by flowing low discharge ($Q = 200 m^3/s$) to the each calculated bed topography after the flood. The calculation results of Case6 indicated that the sediment deposition volume in the middle of the channel from 5.0km to 6.0km was larger than in the results of Case3 and Case5, and the migration of the main channel was clearly shifted to the levees. It can be seen that the large scale sediment deposition in the middle of the channel caused the bed scouring along the left and right banks and the migrations of the main channel. As a result, when the amount of inflow sediment was 7 million (m^3) and the inflow sediment discharge hydrograph which peaked 2 hours before the peak discharge was given at the upstream boundary, the calculation results could reproduce the observed large-scale bed aggradation and channel migration in the lower reach of the river.

5 Conclusions

We found the method of the bed variation analysis in rivers where main channel migrations and large-scale sediment depositions occurred due to a large amount of inflow sediment discharge from mountainous areas. And the inflow sediment discharge hydrograph at the upper boundary was estimated by the introduction of the new concept for the flood flow and bed variation analysis. The developed method was applied to the 1995 record breaking flood of the Hime River and could provide a good explanation for the flood and large scale bed variations.

References

- [1] Kinoshita, R. (1984). "Present status and future prospects of river flow analysis by the aerial photograph". Proceedings of JSCE, No.345, 1-19.
- [2] Hashinoki, T., Mizuyama, T., Satoh, K., and Murakami, M. (2007). "Research on sediment yield and sediment discharge which considers timing of sediment yield". Journal of the Japan Society of Erosion Control Engineering, Volume 59, Issue 5, 15-22.
- [3] Uchida, T. and Fukuoka, S. (2014). "Numerical calculation for bed variation in compound meandering channel using depth integrated model without assumption of shallow water flow". Advances in Water Resources, Volume 72, 45-56.